OPEN ACCESS *International Journal*
Of Modern Engineering Research (IJMER)

Investigation Of Structural Integrity In Circumferential Entry Blades Ofsteam Turbines

A S Suresh Babu[1], M. V. Reddy[2], Jeevan Gowda G[3]
**Ghousia College of Engineering, Ramanagara, India – 562159*
***Professorof Mechanical Engineering, Bangalore Instituteof Technology, India*
****Kshipra Simulations Pvt. Ltd., #48, 5th Main, 4th Cross,RHCS Layout Nagarbhavi, India – 560091*
Corresponding Author : A S Suresh Babu

ABSTRACT:*The bladed disc of an LP last stage rotor assembly in a steam turbine often employs circumferential entry blades. Radial entry blade root design demands for a groove in the disc through which blades are inserted and guided to their respective final positions which alters the stiffness in the disc. spacer is the most highly stressed weak link zonein the circumferential entry rotor disc achieving mechanical integrity for in-service condition is a challenge.*
Challenges prevail in design of circumferential entry blades are achieving parallelism in locking pin, providing contact bearing area in adjacent blades, retaining closing blade/spacer in the disk by providing sufficient gross yielding stress at neck region., edge distance in disk is very sensitive area failure of disk at insertion zone can lead to rotor stage failure.
The present research work focus on structural integrity of spacer during the absence of an airfoilis accomplished through conduction of FE approach along with classical design equations followed by API 616 standards is employed to achieve the mechanical integrity in bladed disc assembly. The structural analysis results of a T-root spacer and a T-root closing blade are compared to highlight the effect of an airfoil on the structural behaviour.
KEYWORDS: *LP stage rotor, steam turbine, centrifugal load, locking pin, spacer.*

Date of Submission: 06-06-2018 Date of acceptance: 21-06-2018

I. INTRODUCTION

Blade failure can be seen in steam turbines often due to the increase in mass flow rate of steam at LP stage, rotor over speeding and manufacturing uncertainties. Such failures result in economic penalties to the affected utilities like blades, disc, nozzle, casing and so on [1]. Circumferential entry type rotor discs are preferable when compared to axial entry bladed discs, as they are designed to withstand high centrifugal forces without the risk of all blades leaving the rotor. This is because in axial entry blades, each blade needs a locking mechanism to hold the blade from moving radially whereas in circumferential entry blades, only closing blade/spacer is the weak link in the rotor. Therefore, if closing blade/spacer is designed for its robustness, the need of locking mechanism for every blade is not necessary. Structural failures in circumferential entry bladed rotors have been commonly seen to occur due to poor design considerations of the locking pin which holds the final closing blade/spacer along with the other adjacent blades together. Inconsistency and errors in manufacturing/assembly also lead to the rotor having significantly lower safety margins. Since, steam turbines have a wide range of applications in industrial power generation, their efficient operating conditions for an extensive period of time is crucial.

The other problems that encountered in closing blade and spaceris eccentricity of hole and pin, fretting, fatigue, vibration, low flow rate. Eccentricity is a condition of loading in which the point of action of load is not on the neutral axis of hole/pin. Whenever there is eccentric loading there starts the effect of combined direct and bending stresses.

Fretting refers to wear and sometimes corrosion damage at the asperities of contact surfaces. This damage is induced under load and in the presence of repeated relative surface motion, as induced for example by vibration. Fretting decreases fatigue strength of materials operating under cycling loading [5]. This can result in fretting fatigue, whereby fatigue cracks can initiate in the fretting zone. Afterwards, the crack propagates into

the material. Experimental work is carried at material testing lab to correlate the FE results for double shear component for benchmarking.

The present research work focus on structural integrity of spacer during the absence of an airfoil is accomplished through conduction of FE approach along with classical design equations followed by API 616 standards is employed to achieve the mechanical integrity in bladed disc assembly. The structural analysis results of a T-root spacer and a T-root closing blade are compared to highlight the effect of an airfoil on the structural behaviour.

II. LOCKINGMECHANISM IN CIRCUMFERENTIAL ENTRY BLADE

The general appearance of a two-pin mounted closing blade and spacer is shown in figure 1. However, this may not hold true for other cases since the number of pins depend on the centrifugal force of the blade at in-service condition, trying to shear the pin.

The T-root closing blade and spaceris plugged at the slot crated in the rotor forinserting and guiding the moving blades. Locking pins are inserted between the closing blade, spacer and adjacent moving blades.

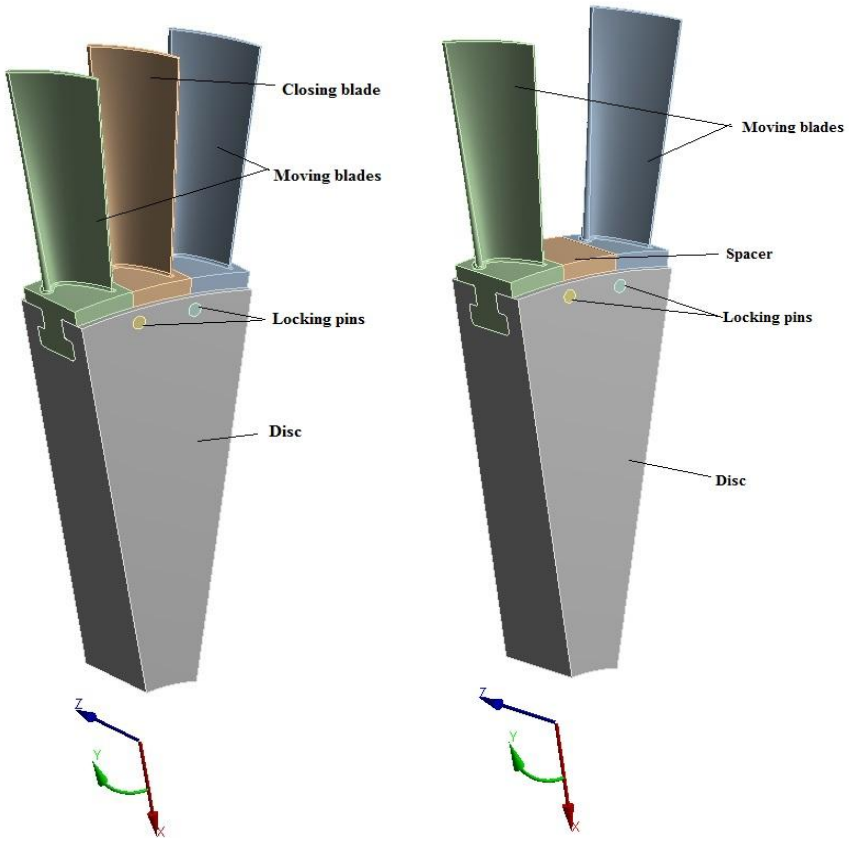

Figure 1: Closing blade and Spacer configuration

The assembly of closing blade/spacer and locking pin is as shown in figure 1. Closing blade is the final blade that is inserted onto the rotor. This blade carries a relatively higher mass than the adjacent blades, since material loss due to presence of holes on either sides of neck region in the closing blade/spacer will result in loss of stiffness and this loss needs to be compensated by increasing the mass of closing blade. The increase in mass will reduce radial growth of pin, which develops friction between blade tip and casing. This friction can be reduced by providing necessary coating to blade tip.Contacts exist between the locking pins and closing blade. These contacts are treated as frictional contacts having coefficient of friction 0.2. There are contacts generated between the blade platforms of closing blade and adjacent blades. These contacts are also treated as frictional contacts with coefficient of friction being 0.2. The locking pins are inserted into the closing blade assembly and a fit is achieved between these bodies through shrink fit. The type of fit achieved between the closing blade and adjacent blades is through tolerance fit. Tolerance of ±10 microns is provided on either sides of the closing blade platform [8]. The stresses created by the steam pressure, centrifugal forces caused by the rotation of the bladed rotor, and the unavoidable vibration resulting in the blading make shot peening [5] an attractive tool to increase the margin between failure and success to an impressive degree.

The other problems that encountered in closing blade is eccentricity of hole and pin, fretting, fatigue, vibration, low flow rate. Eccentricity is a condition of loading in which the point of action of load is not on the neutral axis of hole/pin [10]. The effect of eccentricity causes variation of parallelism in pin which leads to uneven loading on locking pins. The edge distance between rotor and locking is shown in figure 1. The decrease in edge distance will decrease the bearing area between pin and disc which intern increases bearing stress, contact stress at the disc pin interface.

Achieving mechanical integrity of locking blade assembly of design life is a challenge. The material used for blades and rotor is chromium steel (XCrmov55) [6] which is extensively used in manufacture of steam turbine rotors as they are highly corrosion resistant and creep resistant. Similarly, material used for the locking pin is titanium alloy (Ti-6Al-4V) [7] which has high strength, low weight ratio and corrosion resistance. Theanalysis is performed by allocating relevant material properties to components, also considering nonlinearities in geometry and material.

III. EFFECTS OF FRICTION CONTACT MODELLING

The contacts generated in this assembly are all considered to be of frictional type. An isotropic friction model is used in this case which employs a single coefficient of friction μ_{iso} based on the assumption of uniform stick-slip behavior in all directions. From basic Coulomb friction model considered for FE analysis, two contact surfaces can carry shear stresses. When the equivalent shear stress is less than a limiting frictional stressτ_{lim}, there is no motion between the two contact surfaces. This phenomenon is known as sticking. Coulomb friction model is defined as:

$\tau_{lim} = \mu P + b$

$||\tau|| \leq \tau_{lim}$

Where,

τ_{lim} = Limit frictional stress

$||\tau|| = \sqrt{\tau_1{}^2 + \tau_2{}^2}$ equivalent stress (for 3-D contact elements)

μ = coefficient of fiction for isotropic friction

P = normal contact pressure

b = contact cohesion

After the equivalent frictional stress has exceededτ_{lim}, the contact and target surfaces will slide relative with each other. This phenomenon is known as sliding. Figure 2 [9] represents the friction model with respect to sticking and sliding.

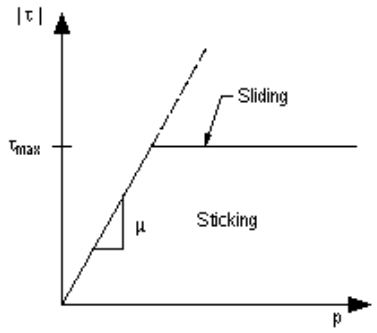

Figure2: Friction model

The friction element geometry for the present is portrayed in figure 3 where R and S axis of the applicable co-ordinate system. Friction element is used to represent contact and sliding between two 3-D target surfaces and a deformable surface defined by eight nodes. is an 8-node element that is intended for general rigid-flexible and flexible-flexible contact analysis and is used to represent contact and sliding between 3-D surfaces. The element is applicable to 3-D structural and coupled field contact analyses. It can degenerate to a six node element depending on the shape of underlying solid elements. Frictionless behaviour allows the bodies to slide relative to one another without any resistance. When friction is included, shear forces can develop between the two bodies.Frictional contact may be used with small-deflection or largedeflectionanalyses.

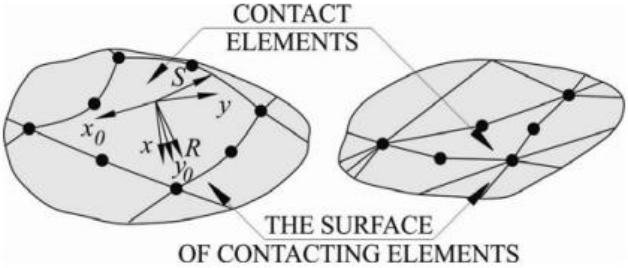

Figure3:Contact Element

The contact element allows the use of both isotropic and orthotropic friction models. In this case an isotropic friction model was used with a variable coefficient ranging between 0.35 and 0.55 and a starting value of 0.45 that corresponds to the coupling materials determined experimentally.

For the finite element, the rate of frictional dissipation is evaluated using the frictional heating factor and is given by

$q = FGTH\tau V$ (1)

where: τ is the equivalent frictional stress,

V – the sliding rate and

FGTH – the fraction of frictional dissipated energy converted into heat (the default value of 1 was used for this parameter).

The amount of frictional dissipation on contact and target surfaces is given by

$qc = FwFf\, tv$ (2)

$qT = (1- Fw)Ff\, tv$ (3)

where: qc - The amount of frictional dissipation on the contact side,

qT - The amount of frictional dissipation on the target side and

FWGT is a weighteddistribution factor (the default value of 0.5 is used for this parameter).

The relationships presented previously are valid only for the sliding mode of friction and a coefficient of friction greater than zero.

IV. LOADSACTING IN CIRCUMFERENTIAL ENTRY ROTOR BLADE

The complete circumferential entry rotor disc and its components are subjected to high rotational velocities, which is a body force. The rotational velocity has an impact on other loading conditions, as bending loads and shear loads are imparted on the locking pins, spacer and closing blade. Shear loads are also prominent along the length of the pins and across the cross section of the pins. However, possibilities of all manufacturaluncertainties like parallelism of locking pin, contact uncertainties likesticking, sliding, partial contact across the length of locking pin. Whenever there is eccentric loading there starts the effect of combined direct and bending stresses. The effect of these loads on the closing blade, spacer and locking pin are therefore investigated through Nonlinear kinematic finite element simulation and customized methodology for theoretical calculations for all design purpose.The design rule margins are necessary for uncertainties present in material, manufacturing, assembly and on site operating conditions.

Yield strength at room temperature = 585 MPa

Yield strength at operating temperature (500) = 575 MPa

Factor of safety at operating speed = 1.68 [11]

Factor of safety at over speed = 1.15 [11]

Allowable stress at operating speed:

$\sigma allowable = \frac{\sigma_{minimu\ m}}{overspeed\ ^2 * FOS}$ (4)

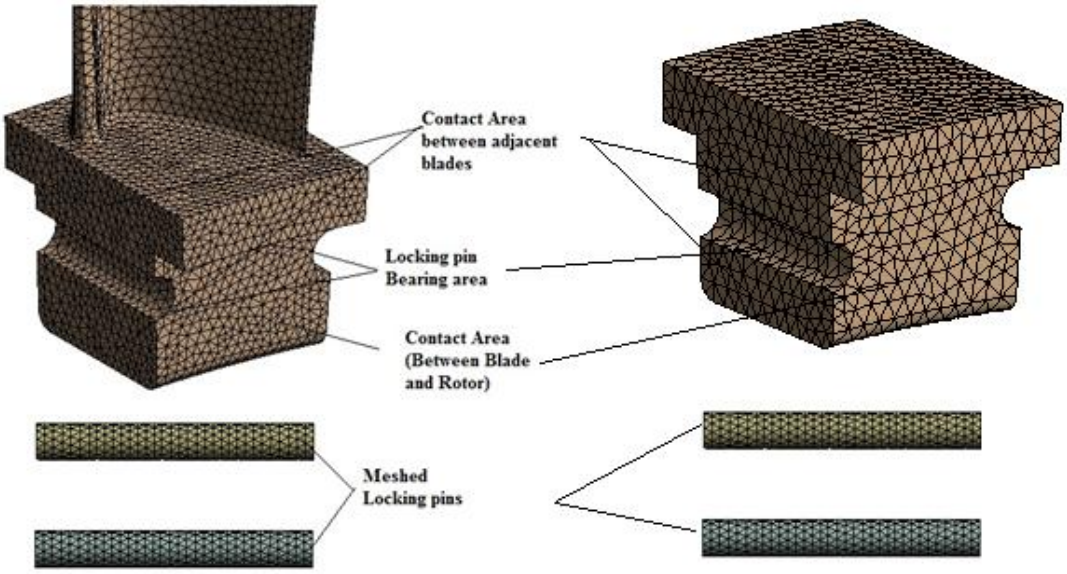

Figure 4: Contact regions in the closing blade and spacer

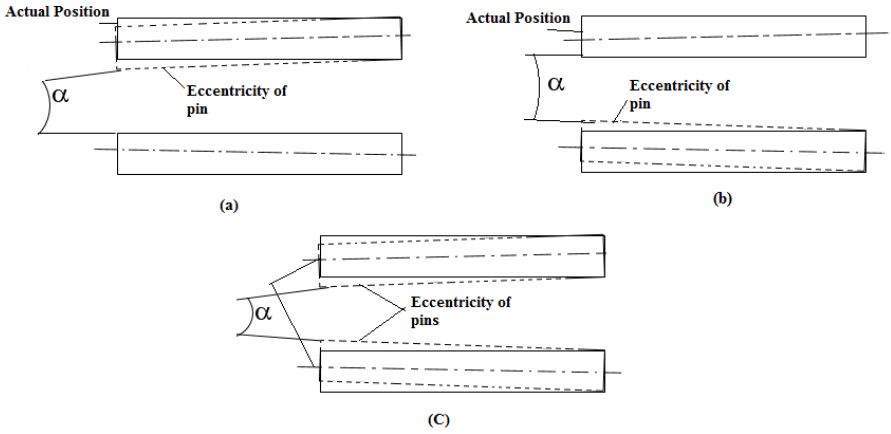

Figure 5: Eccentricity of locking pin

The interactions between blade platforms, the locking pin, spacer and closing blade area of contact, the blades and rotor sliding region are existing under service condition. These junctions of contact, as shown in figure 4 (bodies not to scale) are considered as sensitive contact regions which are subjected to frictional resistance during operation of the turbine. Hence contacts have to be suitably provided with appropriate friction models defined at each location for simulation purposesby updating stiffness for each and every iteration.

The angleα as shown in figure 5 symbolizes the eccentricity of locking pin. The angleα should be equal to zero, hence the load acting on the pin will distribute among locking pins. The eccentricity of pin occurs during assembly due to manufacturing error or variation in tolerances provided resulting in discounting of in-service life.

V. OBJECTIVES AND SCOPE OF WORK

The main objective of this work is to develop a simulation model of the closing blade, spacer and locking pin assembly and conduct sensitivity checks for the bladed disc integrity. Locking pins help in locking the closing blade/spacer which is the final blade being inserted into the rotor.

Being a crucial part in the locking system for the blades, its failure can prove disastrous. The pin is subjected to lateral bending as it holds the closing blade/spacer which is subjected to centrifugal loading due to which it tends to displace in the radial direction. If the bending stresses generated tend to be high, yielding of the pin is inevitable.

Although two locking pins are employed for the locking mechanism in the assembly, it may sometimes not be enough to withstand high and uncertain over speeds.

A comprehensive presentation of structural analysis results of a T-root spacer and a T-root closing

blade are compared to highlight the effect of an airfoil on the structural behaviourthrough sensitivity analysis blending the classical approach with simulation engineering to arrive at best possible solution replicating the physical conditions. Computed engineering analysis could be the best possibility for arriving better clarity at design feasibility during in service conditions.

VI. NUMERICAL INVESTIGATION AND RESULTS

Structural analysis is conducted for the closing blade and spacer assembly for different loading conditions, the geometric variable being the locking pin position. Analysis is also carried out for two different configurations for emplacement of locking pins along the radial direction.

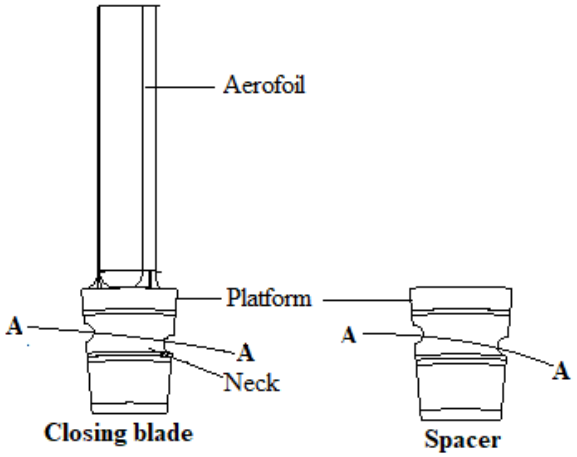

Figure6: Wireframe model of the closing blade and spacer

The neck area and the bearing area in a turbine blade root is subjected to high stress concentration due to large radial forces. During off-design conditions such as over-speed, localized material yield will occur and lead to subsequent blade failure at the neck. Therefore, for the given over-speed of 121% as per API standards, investigation for any structural anomalies is carried out. Critical mean stress is investigated at cross section A-A as shown in figure 6.

VII. CLASSICAL APPROACH FOR SIZING OF LOCKING PIN

Yield Stress, $\sigma_y = \frac{F_C}{A}$N/mm2

Where, σy = Yield strength of titanium alloy = 880 MPa

Centrifugal force, Fc = m$\omega^2 r$

Where, m1 = mass of closing blade = 0.53559 Kg and m2 = mass of spacer = 0.386 Kg

$\omega = \frac{2\pi N}{60}$ rad/sec

r = centre of gravity = 0.419 m

Cross sectional area of locking pin, A = 4A (because, shear of locking pin occurs at 4 regions)

Therefore, diameter of pin = d = 8mm.

Two pins of diameters 8mm are taken for simulation for which both of them are analysed for strength and stresses separately. The neck region of closing blade is a highly stressed as centrifugal loads tend to act directly. Since, the integrity of the locking pins is vital, section stresses at critical locations needs to be below the allowable design stress. Else, failures due to excessive bending and fatigue are inevitable.The results obtained from this simulation are shown in figure 7.

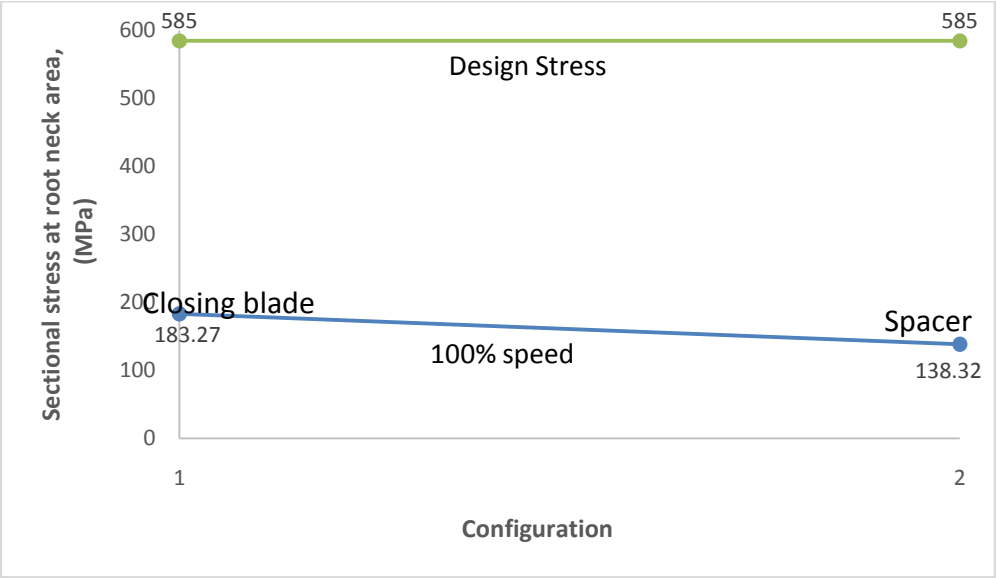

Figure 7: Gross Yielding stress at blade root neck of closing blade and spacer

The neck area and the bearing area in a turbine blade root is subjected to high stress concentration due to large radial forces. It is observed, that section stress at the blade root neck region of configuration 1 is 183.27 MPa whereas for configuration 2 section stress is 138.32 MPa.

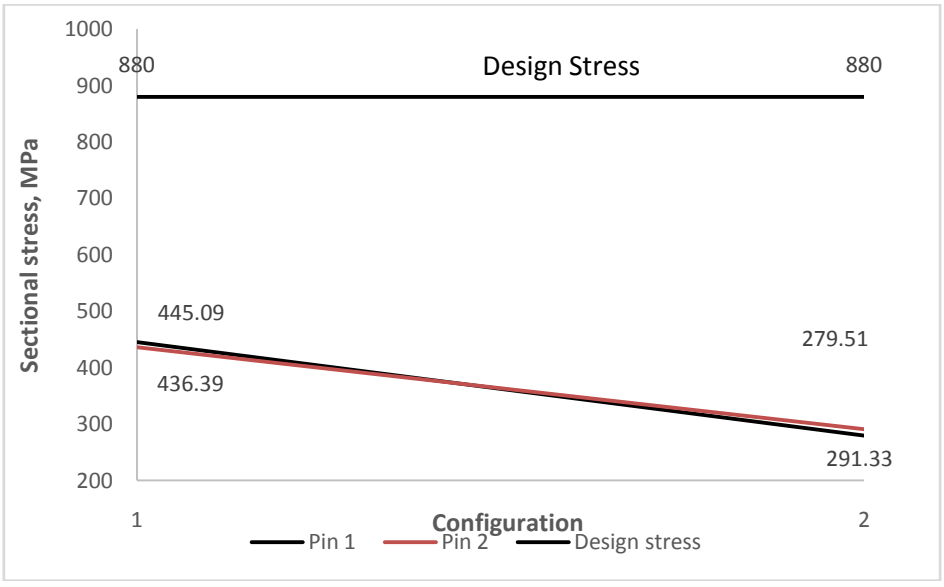

Figure 8: Gross Yielding stress of locking pin in closing blade

In figure 8, the gross yielding stress of configuration 1 (closing blade) is 445.09 MPa and 279.51 MPa in locking pin 1. Similarly, the section stress in locking pin 2 of configuration 1 is 436.39 MPa and 291.33 MPa at different locations as shown in figure 11.
In figure 9, the gross yielding stress of configuration 2 (spacer) is 342.94 MPa and 333.77 MPa in locking pin 1. Similarly, the gross yielding stress in locking pin 2 of configuration 2 is 308.36 MPa and 302.49 MPa. The variation in stress between closing blade and spacer is because of change in mass.

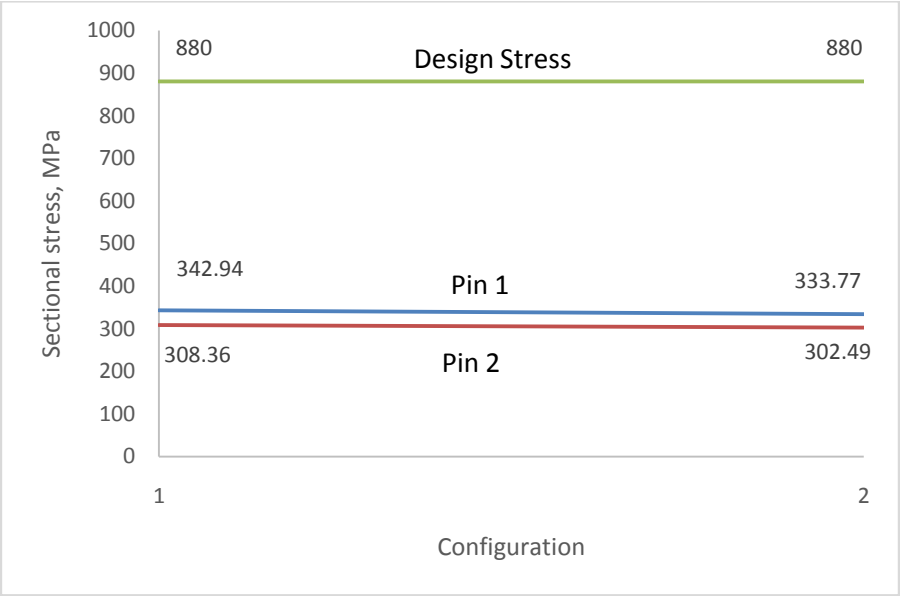

Figure 9: Gross Yielding stress of locking pin in Spacer

VIII. ANALYTICAL VALIDATION

Shear stress is the most common failure method for locking pins as they act as a weak link in the closing blade structure. However, there have been cases of pins failing despite being adequately sized for shear. This may be due to negligence of taking into account pin bending as a legitimate failure mode. Based on simple shear stress equations, the locking pin, spacer and closing blade are investigated and validated through finite element analysis.

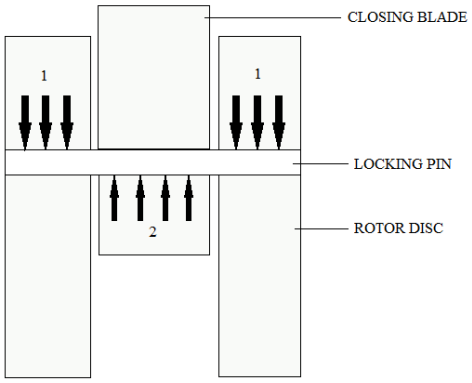

Figure 10: Load distribution across the locking pin

For a closing blade due to its weak link analogy, load distribution across the locking pin is as shown in figure 10 where:

- Load 1 shows variable reactive loads due to the resistance offered by rotor disc.
- Load 2 shows variable load distribution across centre of the locking pin due to centrifugal force exerted on the closing blade and spacer.

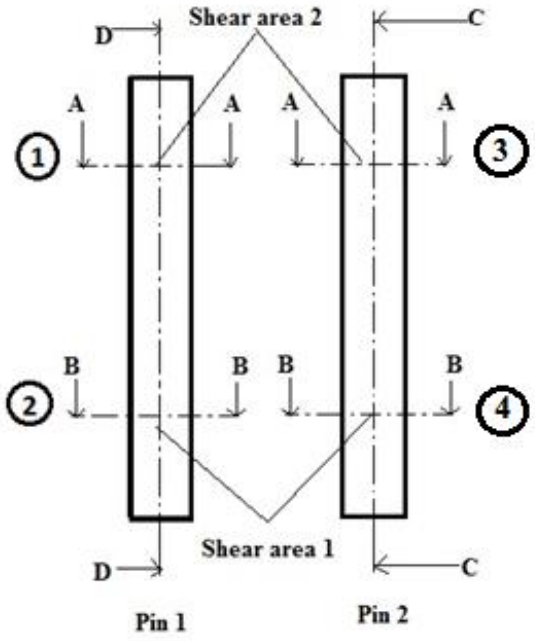

Figure 11: Gross yielding stress at cross sectional area of the locking pin

Stress, $\sigma_y = \frac{F_C}{A}$N/mm2

Centrifugal force, Fc = m$\omega^2 r$

Where, m = mass of closing blade = 0.53559 Kg

$\omega = \frac{2\pi N}{60}$ rad/sec = $\frac{2*\pi*8650}{60}$ = 905.82 rad/sec

r = centre of gravity = 0.419 m

Gross yielding stress in cross section of pin:

For closing blade, Fc = m$\omega^2 r$ = 0.53559 X 905.822 X 0.419 = 184134.82 N

For Spacer, Fc = m$\omega^2 r$ = 0.386 X 905.822 X 0.419 = 132704.34 N

A = $\frac{\pi d^2}{4}$

FOS, Factor of safety = 1.68 [11]

Stress, $\sigma_y = \frac{F_C}{4A} = \frac{184134.82}{201.06}$ = 915.81 N/mm2

Longitudinal shear of pin at cross section D-D and C-C:

For closing blade,

Longitudinal shear $\tau_{pin} = \frac{F_C}{2A} = \frac{184134.82}{960}$ = 191.81 N/mm2

For Spacer,

Longitudinal shear $\tau_{pin} = \frac{F_C}{2A} = \frac{132704.34}{960}$ = 138.23 N/mm2

Shear stress of pin between A-A and B-B:

For closing blade,

Shear stress$\tau_{pin} = \frac{F_C}{2A} = \frac{184134.82}{2*271.39}$ = 339.24 N/mm2

For Spacer,

Shear stress $\tau_{pin} = \frac{F_C}{2A} = \frac{132704.34}{2*271.39}$ = 244.49 N/mm2

(4) Gross yielding stress at cross sectional area of neck region:

For Closing blade,

Stress, $\sigma_y = \frac{F_C}{A} = \frac{184134.82}{1090.81}$ = 168.80 N/mm2 (Cross sectional area at A-A in figure 6)

For spacer,

Stress, $\sigma_y = \frac{F_C}{A} = \frac{132704.34}{1090.81}$ = 121.65 N/mm2 (Cross sectional area at A-A in figure 6)

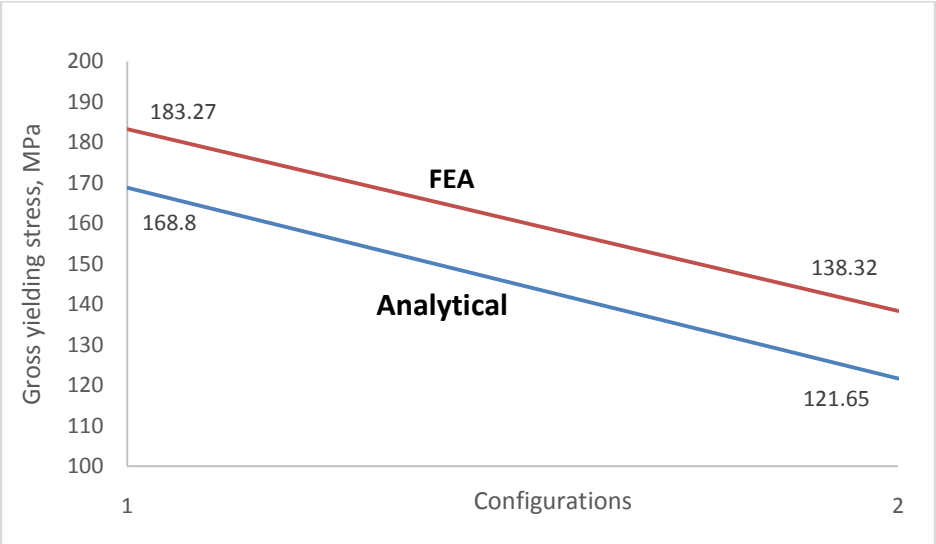

Figure 12: Gross yielding stress at cross sectional area of neck region

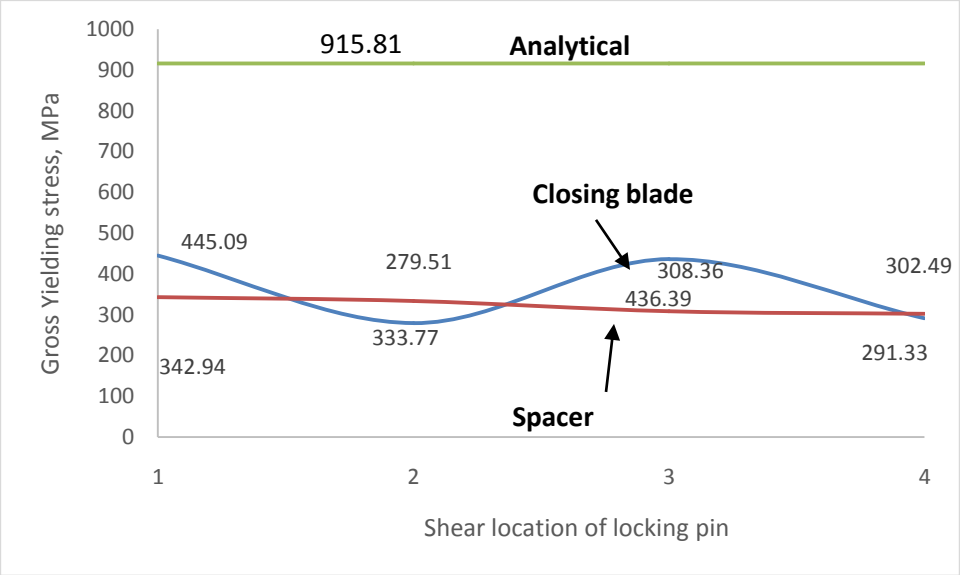

Figure 13: Gross yielding stress at shear area of Locking pins

Figure 13 shows the graphical representation of Gross yielding stress at different cross sectional area of the locking pins as shown in figure 11. The peak stress in locking pin is 445.09 MPa. The variation of gross yielding stress of classical approach from FEA is due to material non linearity, bilinear kinematic hardening, manufacturing uncertainties which are not considered in classical approach.

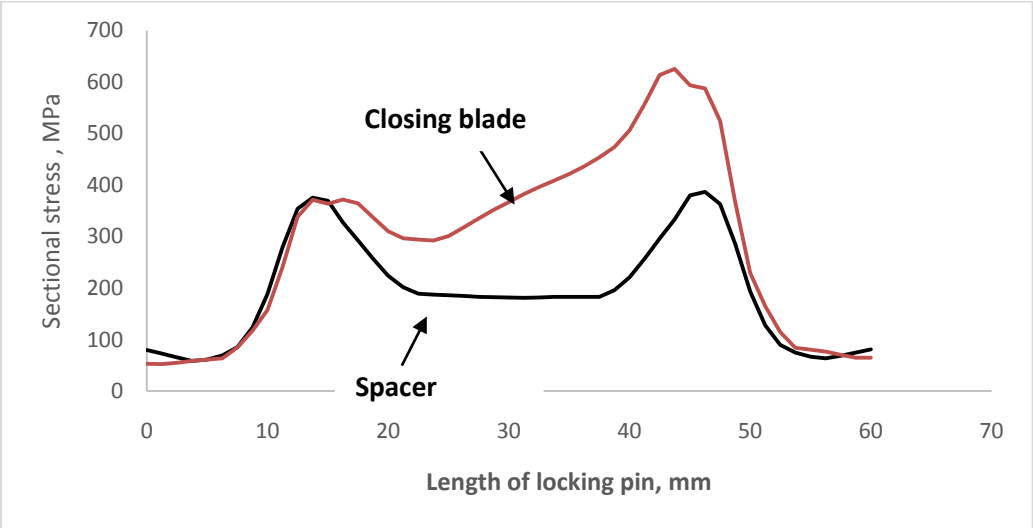

Figure 14: Section stress along the length of locking pin 1

Figure 14 portrays the variation of section stress taken along the length of the locking pin 1(as shown in figure 11 cross-section D-D). The FEA results for section stress along the length of locking pin is obtained from a path. Maximum stress can be observed at a length of 22 mm and 38 mm. This is because at those lengths, there is an interaction between the disc and the locking pin. The locking pin of configuration 2 is less prone to structural weakness as centrifugal force acting on locking pin varies with decrease in mass. The same analogy applies for the second locking pin, where section stress along the length of locking pin 2 (as shown in figure 11 cross-section C-C) is visualized. The results are explained in figure 15 for the locking pin 2in both configurations.

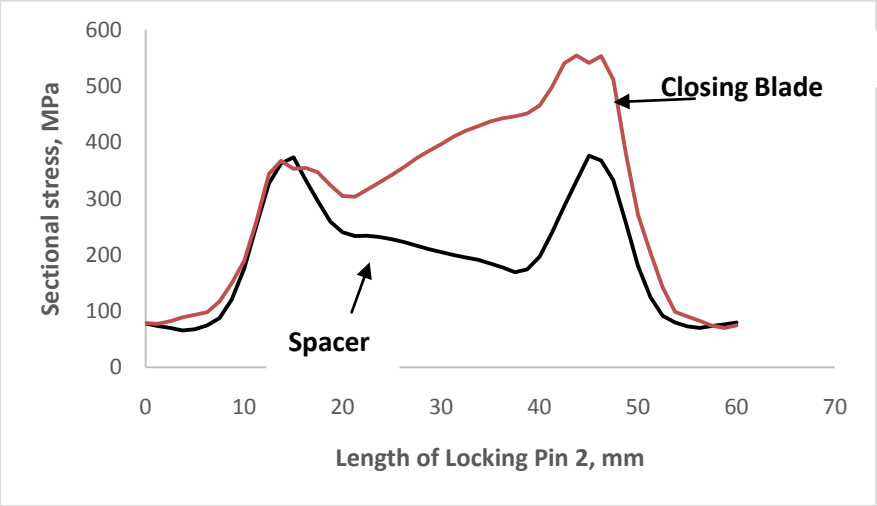

Figure 15: Section stress along the length of locking pin 2

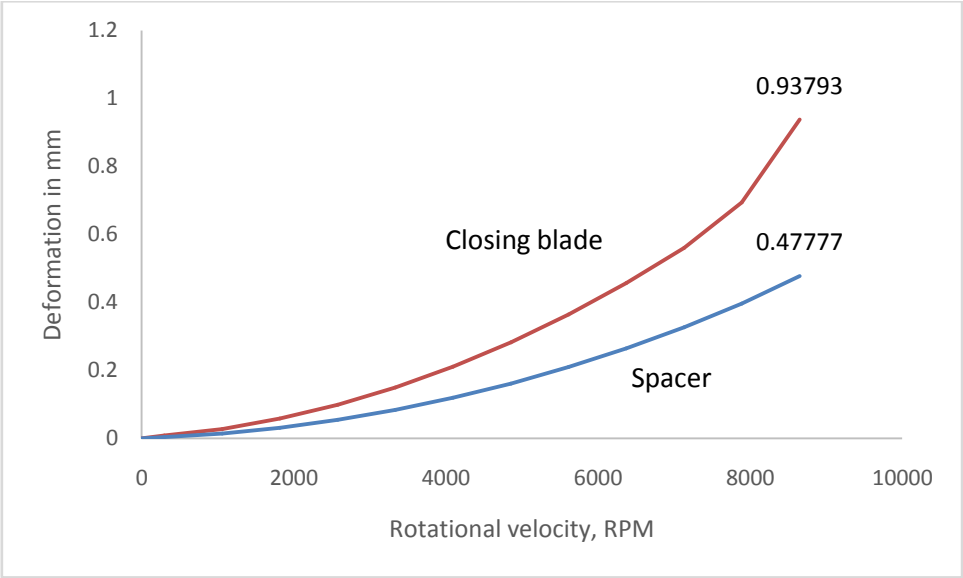

Figure 16: Radial Deformation of Closing blade and spacer

The Graphical representation of radial deformation of closing blade and spacer is as shown in figure 16. Maximum Deformation of closing blade and spacer is 0.93 mm respectively. The radial growth of closing blade is maximum, but the clearance between blade tip and steam turbine casing is 2mm [11]. Hence, both closing blade and spacer are suitable for circumferential locking mechanism.

IX. SHEAR STRESS INVESTIGATION

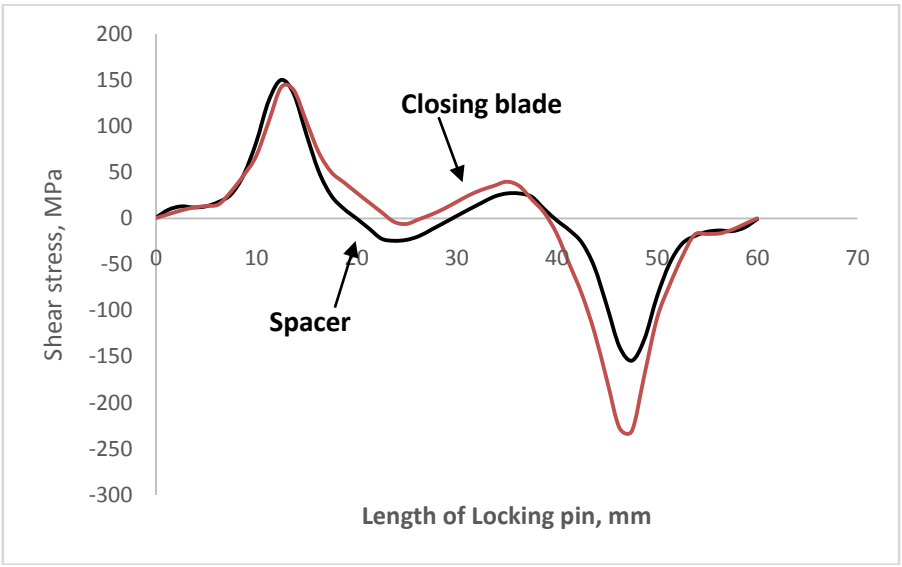

Figure 17: Shear stress along the length of locking pin 1

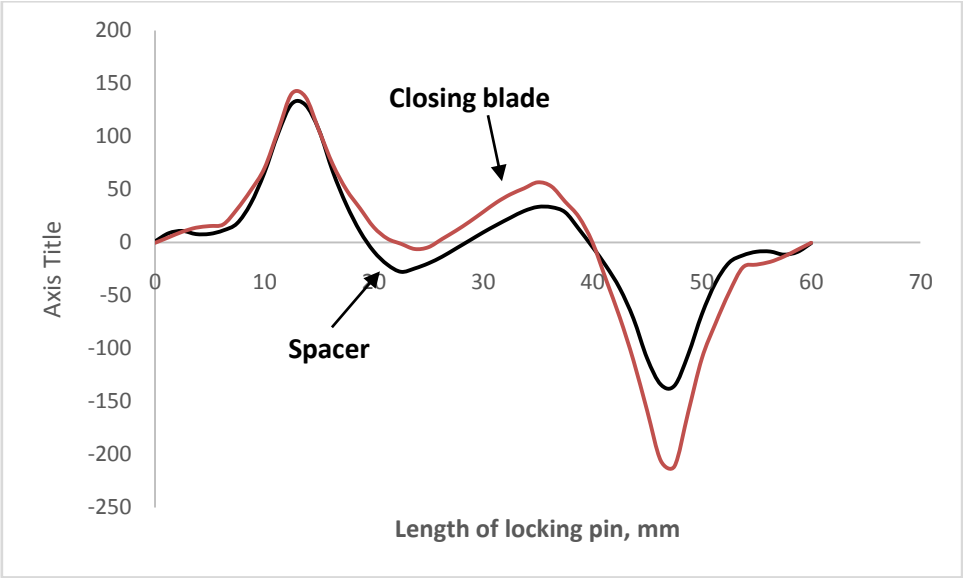

Figure 18: Shear stress along the length of locking pin 2

From shear perspective, the pins are subjected to shear at the disc groove region at 2 locations in each pin. The shear stress distribution in the pins is as shown in the figure 17 and 18. The force distribution that is, the double shear across the pin is shown in figure10. The distribution of stress intensity across the pin is very clearly indicated as expected from the fundamental principles of shear.

X. CONCLUSION

The sensitivity analysis is conducted for circumferential entry blade assembly for different loading conditions blending with classical approach. The Finite element simulation is conducted and best solution is obtained by replicating physical solutions. However, classical approach will not include geometrical nonlinearities, contact elements, manufacturing uncertainties, material nonlinearity and off design conditions.Hence, mathematical model using FEA is conducted and robust design is achieved considering all uncertainties during in-service conditions.

The theoretical classical calculations might yield a greater margin of safety because classical equations do not consider nonlinearity of material and geometry. However, FOS of FE simulation is less than expected outcome because of uncertainties present in material, manufacturing, assembly, on-site operating conditions and Non-linear kinematic analysis.

The study completely reveals the preliminary design considerations to achieve mechanical integrity in circumferential entry blades which can be considered for blade locking mechanisms. The work throws light on achieving an end to end solution for closing blade and spacer considering both bending and shear.

Structural analysis proves that the airfoil in closing blade has contributed towards generation of high magnitudes of stress, bending and bearing area pressure.

The loss of an airfoil does not significantly hinder the stage performance of a turbine which suggests that a spacer can be successfully implemented.

REFERENCES

[1]. E. Poursaeidi, M.R Mohammadi, Failure analysis of lock-pin in a gas turbine engine. Volume 15, Engineering Failure Analysis, Issue 7, October 2008, Pages 847-855.
[2]. Troyanovski, B.M. Steam Turbine Plants, Status, Investigations, Trends. Thermal Engineering, Vol. 36 (1989), No. 2, p.p. 61-67.
[3]. Golinkin, S.L. Reliability of the Steam Turbine Thrust Bearings. Energeticheskoe Mashinostroenie, (Proc. Kharkov State University). Kharkov, 1971, No. 11, p.p. 105-115 (in Russian).
[4]. Leyzerovich, A.Sh. Large Power Steam Turbines: Design and Operation. Penn Well Books, Pennwell Publishing Company, Tulsa, Oklahoma, 1997, Vol. 2, p. 738, Table 8.7.
[5]. Sharma, M. C., and R. K. Joshi. Improvement of fretting fatigue performance of large steam turbine blade material using ball peening. In Proceedings of the second International Conference on Shot Peening and Blast Cleaning (Ed. Sharma, MC), Bhopal, India, pp. 120-130. 2001.
[6]. Rao, J. S., K. Ch Peraiah, and Udai Kumar Singh. Estimation of dynamic stresses in last stage steam turbine blades under reverse flow conditions. Advances in Vibration Engineering, Journal of Vibration Institute of India 8, no. 1 (2009): 71.
[7]. Jaffee, Robert Isaac. Titanium steam turbine blading. In Titanium Steam Turbine Blading, pp. 1-25. 1990.
[8]. Jafarali, P., Dmitry Krikunov, Amir Mujezinović, and Nicholas A. Tisenchek. Probabilistic Analysis of Turbine Blade Tolerancing and Tip Shroud Gap. In ASME Turbo Expo 2012: Turbine Technical Conference and Exposition, pp. 469-476. American Society of Mechanical Engineers, 2012

[9]. ANSYS, Inc, ANSYS Element Reference Guide, Release 16.1, 2016
[10]. Banaszkiewicz, M. A. R. I. U. S. Z. Steam turbines start-ups. Transactions of the Institute of Fluid-Flow Machinery (2014)
[11]. Tulsidas, D., M. Shantharaja, and K. Kumar. Design modification for fillet stresses in steam turbine blade. Int J Adv Eng Technol 3 (2012): 343-346.

A S Suresh Babu "Investigation Of Structural Integrity In Circumferential Entry Blades Ofsteam Turbines"International Journal Of Modern Engineering Research (IJMER), vol. 08, no. 05, 2018, pp.62–75.